Electronic supplementary information for

The effect of phonon modes on the $H_2(v,j)/D_2(v,j)$ - Cu(1nn) scattering processes

Tapas Sahoo, Subhankar Sardar, and Satrajit Adhikari*

Department of Physical Chemistry,

Indian Association for the Cultivation of Science,

Jadavpur, Kolkata -700 032, INDIA

February 13, 2011

I. The 4D⊗2D Time Dependent Discrete Variable Representation (TDDVR) methodology on molecule - surface scattering

As we wish to implement the TDDVR method to solve the above couple Time Dependent Schrödinger Equation (TDSE), the newly formulated methodology for a mean - field type of situation is briefly demonstrated in the simplest but completely generalized way although the detailed formulations of the different versions of TDDVR approach are presented successively elsewhere.[1–15] The basic technical point of TDDVR dynamics is the movement of grid - points (trajectories) by using "classical" equations of motion with time - independent width parameter[3] of the primitive basis set. The form of TDSE in the adiabatic representation for the diatom - surface interaction Hamiltonian for the i th set of molecular DOFs on a single Born -

*Author to whom correspondence should be addressed: Fax: +91-33-2473 2805; Electronic mail: pcsa@iacs.res.in

Oppenheimer surface can be written as the following generalized way:

$$i\hbar\frac{\partial}{\partial t}\Psi_i(\{\chi_k^i\},t) = \hat{H}_i^{eff}(\{\chi_k^i\},t)\Psi_i(\{\chi_k^i\},t), \tag{1}$$

$$\hat{H}_i^{eff}(\{\chi_k^i\},t) = H_i + \langle\Psi_j(\{\chi_k^j\},t)|H_j + \widehat{V}_0(x,y,z,X,Y,Z)|\Psi_j(\{\chi_k^j\},t)\rangle$$

$$+ \langle\Psi_j(\{\chi_k^j\},t)|\widehat{V}_{eff}(x,y,z,X,Y,Z,t,T_s)|\Psi_j(\{\chi_k^j\},t)\rangle,$$

$$i,j = 1,2;\ i \neq j,$$

and

$$\int \Psi_i^\dagger(\{\chi_k^i\},t)\Psi_i(\{\chi_k^i\},t)\prod_{k=1}^{p_i}d\chi_k^i = 1, \tag{2}$$

with $(\{\chi_k^1\} = x,y,z,Z)$ and $(\{\chi_k^2\} = X,Y)$ at any time t. The wavefunction $[\Psi_i(\{\chi_k^i\},t)]$ for the i th set of degrees of freedom (p_i) is expanded in terms of products of TDDVR basis functions $[\{\psi_{l_k}(\chi_k^i,t)\}]$ for the various k th modes,

$$\Psi_i(\{\chi_k^i\},t) = \sum_{l_1 l_2 \ldots l_{p_i}} C^i_{l_1 l_2 \ldots l_{p_i}}(t)\prod_{k=1}^{p_i}\psi_{l_k}(\chi_k^i,t). \tag{3}$$

The l_k th basis for the k th mode is again expressed with DVR basis multiplied by plane wave to represent the coordinate, χ_k^i, as a function of time, t,

$$\psi_{l_k}(\chi_k^i,t) = \phi(\chi_k^i,t)\sum_{n=0}^{N_k}\xi_n^*(x_{l_k})\xi_n(x_k)$$

$$= \sum_{n=0}^{N_k}\xi_n^*(x_{l_k})\Phi_n(\chi_k^i,t),$$

$$\phi(\chi_k^i,t) = \pi^{1/4}\exp\left(\frac{i}{\hbar}\{P_{\bar{\chi}_k^i}(t)[\chi_k^i - \bar{\chi}_k^i(t)]\}\right), \tag{4}$$

where harmonic oscillator eigenfunctions are the primitive basis to construct DVR functions,

$$\xi_n(x_k) = \left(\frac{2ImA_k^i}{\pi\hbar}\right)^{1/4}\frac{1}{\sqrt{n!2^n\sqrt{\pi}}}\exp(-x_k^2/2)H_n(x_k),$$

$$x_k = \sqrt{\frac{2ImA_k^i}{\hbar}}(\chi_k^i - \bar{\chi}_k^i(t)),$$

$$x_{l_k} = \sqrt{\frac{2ImA_k^i}{\hbar}}(\chi_{l_k}^i(t) - \bar{\chi}_k^i(t)). \tag{5}$$

A TDDVR grid - point, $\chi_{l_k}^i$, is determined by eqn (5) using the root, x_{l_k}, of N_k th Hermite polynomial, $H_{N_k}(x_k)$. Since the roots $(x_{l_k}s)$ of the polynomial are fixed values, the positions of

the TDDVR grid - points ($\chi_{l_k}^i$s) will change as a function of time due to the time - dependent variables, $\bar{\chi}_k^i(t)$,

$$\chi_{l_k}^i(t) = \bar{\chi}_k^i(t) + \sqrt{\frac{\hbar}{2ImA_k^i}} x_{l_k}. \tag{6}$$

The Gauss - Hermite basis, $\Phi_n(\chi_k^i, t)$, for the k th mode as introduced in eqn (4), have the following important properties: (a) They form an orthonormal basis,

$$\int d\chi_k^i \Phi_m^*(\chi_k^i, t)\Phi_n(\chi_k^i, t) = \delta_{mn}^k, \tag{7}$$

(b) The ground state of the G - H basis is a Gaussian Wave Packet.

The TDDVR basis functions, ψ_{l_k} s, as defined in eqn (3) for the k th mode constitute an orthogonal but not normalized set,

$$\int d\chi_k^i \psi_{l_k}^*(\chi_k^i, t)\psi_{l_k'}(\chi_k^i, t) = \delta_{l_k l_k'} A_{l_k l_k'}, \tag{8}$$

where A_k is the normalization factor.

When the molecule - surface interaction Hamiltonian [see eqn (2) in main text] and the TDDVR representation of wavefunction [eqns (3), (4), (5)] are substituted into the TDSE [eqn (1)], the classical path picture appears naturally along with the quantum equation of motion. The compact form of TDDVR matrix equation for quantum motion can be obtained by employing time - dependent variational principle[16] as given below:

$$i\hbar \mathbf{A}\dot{\mathbf{C}}^{\mathbf{i}} = \mathbf{H}_{\mathbf{t}}^{\mathbf{i}}\mathbf{C}^{\mathbf{i}}, \tag{9}$$

and the matrix equation under a similarity transformation takes the following convenient form,

$$i\hbar \dot{\mathbf{D}}^{\mathbf{i}}(\mathbf{t}) = \mathbf{A}^{-1/2}\mathbf{H}_{\mathbf{t}}^{\mathbf{i}}\mathbf{A}^{-1/2}\mathbf{D}^{\mathbf{i}}, \tag{10}$$

where $\mathbf{D}^{\mathbf{i}} = \mathbf{A}^{1/2}\mathbf{C}^{\mathbf{i}}$.

The explicit expression of the differential equation ($i\hbar \dot{\mathbf{D}}^{\mathbf{i}}(\mathbf{t}) = \mathbf{A}^{-1/2}\mathbf{H}_{\mathbf{t}}^{\mathbf{i}}\mathbf{A}^{-1/2}\mathbf{D}^{\mathbf{i}}$) for an ampli-

tude, $d^i_{l_1 l_2 \ldots l_{p_i}}$ is,

$$
\begin{aligned}
i\hbar \dot{d}^i_{l_1 l_2 \ldots l_{p_i}} &= \frac{1}{2}\Big\{ \sum_k \dot{P}_{\bar{\chi}^i_k} \sqrt{\frac{\hbar}{ImA^i_k}} \bar{G}_{l_k l_k} \Big\} d^i_{l_1 l_2 \ldots l_{p_i}} - \Big\{ \sum_k \frac{\mu(\dot{\bar{\chi}}^i_k)^2}{2} \Big\} d^i_{l_1 l_2 l \ldots l_{p_i}} \\
&+ \sum_k \Big\{ \frac{\hbar ImA^i_k}{2\mu} \sum_{l'_1 l'_2 \ldots l'_{p_i}} \bar{F}_{l_k l'_k} d^i_{l'_1 l'_2 \ldots l'_{p_i}} \prod_{k' \neq k}^{p_i} \delta_{l_{k'_i} l'_{k'_i}} \Big\} \\
&+ i\Big\{ \sum_k (\dot{P}_{\bar{\chi}^j_k})^2 \sqrt{\hbar ImA^j_k} \sum_{m'_1 m'_2 \ldots m'_{p_j}} d^{j*}_{m'_1 m'_2 \ldots m'_{p_j}} \\
&\qquad \sum_{m_1 m_2 \ldots m_{p_j}} d^j_{m_1 m_2 \ldots m_{p_j}} \bar{W}_{m'_k m_k} \prod_{k' \neq k}^{p_j} \delta_{m_{k'_j} m'_{k'_j}} \cdot d^i_{l_1 l_2 \ldots l_{p_i}} \Big\} \\
&+ \Big\{ \sum_k \frac{\mu(\dot{\bar{\chi}}^j_k)^2}{2} \Big\} \sum_{m_1 m_2 \ldots m_{p_j}} |d^j_{m_1 m_2 \ldots m_{p_j}}|^2 \cdot d^i_{l_1 l_2 \ldots l_{p_i}} \\
\\
&+ \sum_k \Big\{ \frac{\hbar ImA^j_k}{2\mu} \sum_{m'_1 m'_2 \ldots m'_{p_j}} d^{j*}_{m'_1 m'_2 \ldots m'_{p_j}} \\
&\qquad \sum_{m_1 m_2 \ldots m_{p_j}} d^j_{m_1 m_2 \ldots m_{p_j}} \bar{F}_{m_k m'_k} \prod_{k' \neq k}^{p_j} \delta_{m_{k'_j} m'_{k'_j}} \cdot d^i_{l_1 l_2 \ldots l_{p_i}} \Big\} \\
&+ \sum_{m_1 m_2 \ldots m_{p_j}} |d^j_{m_1 m_2 \ldots m_{p_j}}|^2 \cdot V_0(\chi_{l_1} \chi_{l_2} \cdots \chi_{l_{p_i}}, \chi_{m_1} \chi_{m_2} \cdots \chi_{m_{p_j}}) \cdot d^i_{l_1 l_2 \ldots l_{p_i}} \\
&+ \sum_{m_1 m_2 \ldots m_{p_j}} |d^j_{m_1 m_2 \ldots m_{p_j}}|^2 \cdot V_{eff}(\chi_{l_1} \chi_{l_2} \cdots \chi_{l_{p_i}}, \chi_{m_1} \chi_{m_2} \cdots \chi_{m_{p_j}}, t, T_s) \cdot d^i_{l_1 l_2 \ldots l_{p_i}}
\end{aligned}
$$

$$(11)$$

where

$$\bar{G}_{l_k,l'_k} = \frac{G_{l_k,l'_k}}{\sqrt{A_{l_k,l_k}A_{l'_k,l'_k}}}, \quad \bar{F}_{l_k,l'_k} = \frac{F_{l_k,l'_k}}{\sqrt{A_{l_k,l_k}A_{l'_k,l'_k}}}, \quad \bar{W}_{l_k,l'_k} = \frac{W_{l_k,l'_k}}{\sqrt{A_{l_k,l_k}A_{l'_k,l'_k}}},$$

$$d^i_{l_1 l_2 \ldots l_{p_i}} = C^i_{l_1 l_2 \ldots l_{p_i}} \prod_{k=1}^{p_i} (A_{l_k,l_k})^{\frac{1}{2}},$$

$$A_{l_k,l'_k} = \sum_{n=0}^{N_k} \xi^*_n(x_{l_k})\xi_n(x_{l'_k}),$$

$$G_{l_k,l'_k} = \sum_{n=0}^{N_k-1} \xi^*_{n+1}(x_{l_k})\sqrt{n+1}\xi_n(x_{l'_k}) + \sum_{n=1}^{N_k} \xi^*_{n-1}(x_{l_k})\sqrt{n}\xi_n(x_{l'_k}),$$

$$F_{l_k,l'_k} = \sum_{n=0}^{N_k-2} \xi^*_{n+2}(x_{l_k})\sqrt{(n+1)(n+2)}\xi_n(x_{l'_k}) + \sum_{n=2}^{N_k} \xi^*_{n-2}(x_{l_k})\sqrt{n(n-1)}\xi_n(x_{l'_k})$$

$$- \sum_{n=0}^{N_k} \xi^*_n(x_{l_k})(2n-1)\xi_n(x_{l'_k})$$

$$W_{l_k,l'_k} = \sum_{n=0}^{N_k-1} \xi^*_{n+1}(x_{l_k})\sqrt{n+1}\xi_n(x_{l'_k}) - \sum_{n=1}^{N_k} \xi^*_{n-1}(x_{l_k})\sqrt{n}\xi_n(x_{l'_k}), \tag{12}$$

The TDDVR equation of motion for quantum dynamics has the following important characteristics: (a) The component matrices ($\{\mathbf{A_k}\}$, $\{\mathbf{G_k}\}$, $\{\mathbf{F_k}\}$, $\{\mathbf{W_k}\}$) of the TDDVR Hamiltonian matrix [see eqn (11)] are time - independent and need to be evaluated once for all. It may be noted that the matrices, $\{\mathbf{A_k}\}$, $\{\mathbf{G_k}\}$ and $\{\mathbf{F_k}\}$ are symmetric hermitian, whereas the matrix, $\{\mathbf{W_k}\}$, is antisymmetric but becomes hermitian with its' prefactor, $i(= \sqrt{-1})$; (b) Since the matrices, $\{\mathbf{G_k}\}$, are diagonal and associated with the "classical" variables $\{\dot{P}_{\bar{\chi}^i_k}(t)\}$, the non - linear dynamics of these "classical" quantities affects the convergence but not the final solution of the quantum equations of motion; (c) As the off - diagonal elements of $\{\mathbf{F_k}\}$ and $\{\mathbf{W_k}\}$ matrices couple the grid - points and dominate the quantum dynamics, any non - linear "classical" propagation of their associated parameter, $\{ImA^i_k\}$, is not desirable, and hence, a time - independent width parameters are the obvious choice; (d) The contribution of different modes on a time - dependent amplitude ($\dot{d}^i_{l_1 l_2 \ldots l_{p_i}}$) can be evaluated independently, i.e., $\mathbf{F_k}$ and $\mathbf{W_k}$ matrices couple grid - points or basis functions of the k th mode. This feature allows parallelization of the algorithm, reduces computational cost remarkably and paves the possibility to pursue relatively large dimensional calculations.

On the other hand, the classical path equations for the k th mode, those appear along with the

quantum equation of motion, can be written as

$$\dot{\chi}_k^i(t) = \frac{P_{\bar{\chi}_k^i}(t)}{m_k} \tag{13}$$

$$\dot{P}_{\bar{\chi}_k^i}(t) = -\frac{dV(\{\chi_k^i\})}{d\chi_k^i}\Big|_{\chi_k^i(t)=\bar{\chi}_k^i(t)} + \chi_k^{i,F}(t), \tag{14}$$

where m_k is either the reduced (μ) or the total (M) mass of the diatom and $\chi_k^{i,F(t)}$ is the quantum force. A rigorous expression of the quantum force, $\chi_k^{i,F(t)}$ for the "classical" equation of motion is derived by using Dirac - Frenkel variational principle,[16] i.e., by minimizing the following integral with respect to $\dot{P}_{\bar{\chi}_k^i}$,

$$I_i = \int \left(-i\hbar \frac{\partial \Psi_i^*(\{\chi_k^i\}, t)}{\partial t} - H(\{P_{\chi_k^i}\}, \{\chi_k^i\})\Psi_i^*(\{\chi_k^i\}, t)\right)$$

$$\times \ \left(i\hbar \frac{\partial \Psi_i(\{\chi_k^i\}, t)}{\partial t} - H(\{P_{\chi_k^i}\}, \{\chi_k^i\})\Psi_i(\{\chi_k^i\}, t)\right) \prod_{k=1}^{p_i} d\chi_k^i. \tag{15}$$

The explicit expression of $\chi_k^{i,F}(t)$ thus obtained is

$$\chi_k^{i,F}(t) = \sum_{l_1 l_2..l_k l_k'..l_{p_i}} C_{l_1 l_2..l_k..l_{p_i}}^{i*}(t) C_{l_1 l_2..l_k'..l_{p_i}}^{i}(t)$$

$$\times \ \left\{ \frac{2(ImA_k^i)^2}{\mu}\left[S_{l_k l_k'}^{(2)} \frac{S_{l_k l_k}^{(1)*}}{A_{l_k l_k}} - S_{l_k l_k'}^{(3)}\right] - \frac{\hbar ImA_k^i}{\mu}\left[R_{l_k l_k'}\frac{S_{l_k l_k}^{(1)*}}{A_{l_k l_k}} - T_{l_k l_k'}^*\right]\right\}$$

$$/ \ \left[\sum_{l_1 l_2..l_k..l_{p_i}} C_{l_1 l_2..l_k..l_{p_i}}^{i*}(t) C_{l_1 l_2..l_k..l_{p_i}}^{i}(t)\frac{S_{l_k l_k}^{(1)*} S_{l_k l_k}^{(1)}}{A_{l_k l_k}}\right.$$

$$- \sum_{l_1 l_2..l_k l_k'..l_{p_i}} C_{l_1 l_2..l_k..l_{p_i}}^{i*}(t) C_{l_1 l_2..l_k'..l_{p_i}}^{i}(t)S_{l_k l_k'}^{(2)*}\bigg], \tag{16}$$

where

$$R_{l_k l_k'} = \sum_p \xi_p^*(x_{l_k})\xi_p(x_{l_k'})2p$$

$$S_{l_k l_k'}^{(n)} = \sum_{pq} \xi_p^*(x_{l_k})\xi_q(x_{l_k'}) \int \Phi_q^*(\chi_k, t)(\chi_k - \bar{\chi}_k^i(t))^n \Phi_p(\chi_k, t)d\chi_k^i$$

$$T_{l_k l_k'} = \sum_{pq} \xi_p(x_{l_k})\xi_q^*(x_{l_k'})2p \int \Phi_p^*(\chi_k, t)(\chi_k - \bar{\chi}_k^i(t))\Phi_q(\chi_k^i, t)d\chi_k^i \tag{17}$$

with

$$\int \Phi_p^*(\chi_k^i, t)(\chi_k^i - \bar{\chi}_k^i(t))\Phi_q(\chi_k^i, t)d\chi_k^i = \frac{1}{2}\sqrt{\frac{\hbar}{ImA_k^i}}\{\sqrt{p+1}\delta_{p+1,q} + \sqrt{p}\delta_{p-1,q}\}$$

$$\int \Phi_p^*(\chi_k^i, t)(\chi_k^i - \bar{\chi}_k^i(t))^2\Phi_q(\chi_k^i, t)d\chi_k^i = \frac{\hbar}{4ImA_k^i} \times \{\sqrt{(p+1)(p+2)}\delta_{p+2,q}$$

$$+ \quad (2p+1)\delta_{p,q} + \sqrt{p(p-1)}\delta_{p-2,q}\}$$

$$\int \Phi_p^*(\chi_k^i, t)(\chi_k^i - \bar{\chi}_k^i(t))^3\Phi_q(\chi_k^i, t)d\chi_k^i = \frac{1}{8}(\frac{\hbar}{ImA_k^i})^{3/2} \times \{\sqrt{(p+1)(p+2)(p+3)}\delta_{p+3,q}$$

$$+ \quad 3(p+1)\sqrt{p+1}\delta_{p+1,q} + 3p\sqrt{p}\delta_{p-1,q}$$

$$+ \quad \sqrt{p(p-1)(p-2)}\delta_{p-3,q}\}. \tag{18}$$

Matrices R, $S^{(n)}$, T and A are time - independent and need to be calculated once for all the time. It is important to note that the time - dependence of $\chi_k^{i,F}$ arises from the time - dependent coefficients $\{C_{l_1 l_2..l_k..l_{p_i}}^i(t)\}$ only.

II. Propagation and Projection

The initial wavefunction [eqn (18a) in the main text] can be expressed in terms of TDDVR basis functions as given below:

$$\Psi_1(x, y, z, Z, t_0) = \sum_{IJKL} C_{IJKL}^1(t_0)\psi_I(x)\psi_J(y)\psi_K(z)\psi_L(Z),$$

$$= \frac{1}{r}g_v(r)Y_{jm_j}(\theta, \phi)\Phi_{GWP}(Z, t_0). \tag{19}$$

If we define the amplitude of the wavefunction only at the TDDVR grid points, the function takes the following form due to orthogonality relationship of the basis functions known at the grid points:

$$\Psi_1(x_I, y_J, z_K, Z_L, t_0) = \frac{C_{IJKL}^1(t_0)}{ImA}A_{II}^x A_{JJ}^y A_{KK}^z A_{LL}^Z,$$

$$= \frac{g_v(r_{IJK})}{r_{IJK}}Y_{jm_j}(\theta_{IJK}, \phi_{IJK})\Phi_{GWP}(Z_L, t_0), \tag{20}$$

which in turn gives the following expression for the initial amplitude of the wavefunction:

$$d_{IJKL}^1(t_0) = ImA\frac{\frac{1}{r_{IJK}}g_v(r_{IJK})Y_{jm_j}(\theta_{IJK}, \phi_{IJK})}{\sqrt{A_{II}^x A_{JJ}^y A_{KK}^z A_{LL}^Z}}\Phi_{GWP}(Z_L, t_0), \tag{21}$$

where $ImA = \left(\frac{\hbar}{2}\right)(ImA_x ImA_y ImA_z ImA_Z)^{-\frac{1}{4}}$.

When we wish to calculate energy resolved state-to-state transition probabilities, we need to project on the product of plane waves, vibrational wave functions of a Morse oscillator ($g_v(r)$) and wave functions of spherical harmonics ($Y_{j',m'_j}(\theta, \phi)$),

$$
\begin{aligned}
\Psi(x,y,z,Z,t) &= \sum_{k'_{out},v',j',m'_j} C^+_{k'_{out},v',j',m'_j}(t) \frac{1}{\sqrt{2\pi}} \exp[ik'_{out}Z] \frac{1}{r} g_{v'}(r) Y_{j',m'_j}(\theta,\phi) \\
&= \sum_{IJKL} C_{IJKL}(t) \sum_P \Phi_P(\xi^x_I)\Phi(\xi^x) \sum_Q \Phi_Q(\xi^y_J)\Phi(\xi^y) \\
&\times \sum_R \Phi_R(\xi^z_K)\Phi(\xi^z) \sum_S \Phi_S(\xi^Z_L)\Phi(\xi^Z)
\end{aligned}
\tag{22}
$$

Multiplying both side by $\frac{1}{\sqrt{(2\pi)}} \exp[-ik_{out}Z] \frac{1}{r} g_v Y^*_{j,m_j}(\theta,\phi)$ in eqn (22) and then, integrating over $d\xi^x d\xi^y d\xi^z d\xi^Z$, we produce the simplified form of the expansion coefficient ($C^+_{k_{out},v,j,m_j}(t)$):

$$
\begin{aligned}
C^+_{k_{out},v,j,m_j}(t) &= \frac{1}{\sqrt{2\pi}} \sum_{IJKL} C_{IJKL}(t) \sum_{PQR} \Phi^*_P(\xi^x_I)\Phi^*_Q(\xi^y_J)\Phi^*_R(\xi^z_K) \\
&\times \iiint \frac{1}{r} g_v(r) Y^*_{j,m_j}(\theta,\phi) \Phi_P(\xi^x)\Phi_Q(\xi^y)\Phi_R(\xi^z) d\xi^x d\xi^y d\xi^z \\
&\times \sum_S \Phi^*_S(\xi^Z_L) \int \exp[-ik_{out}Z] \Phi_S(\xi^Z) d\xi^Z
\end{aligned}
\tag{23}
$$

Since $\int d\xi^k \Phi^*_m(\xi^k)\Phi_m(\xi^k) = 1$, and approximately we have $\int d\xi^k \to \sum_i 1/A^k_{ii}$ at the roots (ξ^k_i) of the Hermite polynomial, we can further modify eqn (23) as:

$$
\begin{aligned}
C^+_{k_{out},vjm_j}(t) &= \frac{1}{\sqrt{2\pi}}(ImA) \sum_{IJKL} \left(\frac{d_{IJKL}}{\sqrt{A^x_{II} A^y_{JJ} A^z_{KK} A^Z_{LL}}} \right) \\
&\times \frac{1}{r_{IJK}} g_v(r_{IJK}) Y^*_{jm_j}(\theta_{IJK},\phi_{IJK}) \exp(-ik_{out}Z_L) \\
&\times \exp\left\{ \frac{i}{\hbar}[P^Z_{s_c}(Z_L - Z_c)] \right\},
\end{aligned}
\tag{24}
$$

Similarly, we derive the expression of the incoming flux at zero time as:

$$
\begin{aligned}
C^-_{k_{in},vjm_j}(t_0) &= \left(\frac{2}{\pi}\right)^{1/4} (ImA)\sqrt{\Delta_Z} \exp[i(k_{in}-k_0)Z_c - \Delta^2_Z(k_{in}-k_0)^2] \\
&\times \frac{\frac{1}{r_{IJK}} g_v(r_{IJK}) Y_{jm_j}(\theta_{IJK},\phi_{IJK})}{\sqrt{A^x_{II} A^y_{JJ} A^z_{KK}}}.
\end{aligned}
\tag{25}
$$

where k_{in} and k_{out} indicate the incoming and outgoing wave vectors, respectively.

III. A "stochastic" treatment for the formulation of phonon energy transfer

The energy transfer from the incoming molecule to the solid is given by:

$$\Delta E_{Ph} = \sum_k \sum_{n_k} \sum_{n_k^0} p_{n_k^0}(E_{n_k} - E_{n_k^0})P_{n_k^0 \rightarrow n_k}, \tag{26}$$

where $P_{n_k^0 \rightarrow n_k}$ is the k th mode transition probability from quantum state n_k^0 to n_k of a Linearly Forced Harmonic Oscillator (LFHO) and the "stochastic" treatment[20,21] of such model provides the following form of transition probability in terms of modified Bessel function (I_0):

$$P_{n_k^0 \rightarrow n_k} = \frac{1}{\rho_k}\exp[-(n_k + n_k^0 + 1)/\rho_k] \times I_0\left[\frac{2}{\rho_k}\sqrt{(n_k + \frac{1}{2})(n_k^0 + \frac{1}{2})}\right], \tag{27}$$

within the harmonic approximation, the following energy difference between the two quantum states appears as:

$$E_{n_k} - E_{n_k^0} = \hbar\omega_k(n_k - n_k^0), \tag{28}$$

and the occupation probability, $p_{n_k^0}$, in the n_k^0 th state for the k th mode at temperature, T_s could be determined either by Boltzmann [Eq. (9)] or by Bose - Einstein [Eq. (10)] probability factor.

We divide the contribution for phonon excitation ($n_k \geq n_k^0$), ΔE_{Ph}^+ and de - excitation ($n_k < n_k^0$), ΔE_{Ph}^-, consider **Boltzmann probability (BP) factor** for the initial state distribution and substitute Eq. (9), (27) and (28) in the Eq. (26) to obtain:

$$\begin{aligned}\Delta E_{Ph}^+ &= \sum_k \hbar\omega_k\rho_k^{-1}(1 - z_k)\sum_{n_k}\sum_{n_k^0} z_k^{n_k^0}(n_k - n_k^0) \\ &\times \exp[-(n_k + n_k^0 + 1)/\rho_k] \times I_0\left[\frac{2}{\rho_k}\sqrt{(n_k + \frac{1}{2})(n_k^0 + \frac{1}{2})}\right],\end{aligned} \tag{29}$$

which can be simplified to

$$\begin{aligned}\Delta E_{Ph}^+ &= \sum_k \hbar\omega_k\rho_k^{-1}(1 - z_k)\sum_{m}\sum_{n_k^0} z_k^{n_k^0} m\exp(-\frac{m}{\rho_k}) \\ &\times \exp[-(2n_k^0 + 1)/\rho_k] \times I_0\left[\frac{2}{\rho_k}\sqrt{(m + n_k^0 + \frac{1}{2})(n_k^0 + \frac{1}{2})}\right],\end{aligned} \tag{30}$$

with $m = n_k - n_k^0$. The double sum in Eq. (30) can be replaced by a double integral to bring an intermediate result:

$$\Delta E_{Ph}^+ = \sum_k \hbar\omega_k \rho_k^{-1}(1 - z_k) \int_0^\infty dm\, m \int_0^\infty dn_k^0\, z_k^{n_k^0}$$

$$\times \quad \exp[-(2n_k^0 + 1 + m)/\rho_k] \times I_0\left[\frac{2}{\rho_k}\sqrt{(m + n_k^0 + \frac{1}{2})(n_k^0 + \frac{1}{2})}\right], \qquad (31)$$

which turns into the following expression under substitution, $x = n_k^0 + \frac{1}{2}$:

$$\Delta E_{Ph}^+ = \sum_k \hbar\omega_k z_k^{-\frac{1}{2}} \rho_k^{-1}(1 - z_k) \int_0^\infty dm\, m \int_0^\infty dx\, z_k^x \exp[-(2x + m)/\rho_k] \times I_0\left[\frac{2}{\rho_k}\sqrt{(m + x)x}\right]$$

$$= \sum_k \hbar\omega_k z_k^{-\frac{1}{2}} \rho_k^{-1}(1 - z_k) \int_0^\infty dm\, m \exp(-\frac{m}{\rho_k}) \int_0^\infty dx\, z_k^x \exp(-\frac{2x}{\rho_k}) \times I_0\left[\frac{2}{\rho_k}\sqrt{(m + x)x}\right].$$

$$(32)$$

The last part of the above integral can be calculated using the following standard integral[22]

$$\int_0^\infty dy\, \exp(-\alpha y)\, \times I_0(\beta\sqrt{y^2 + 2\gamma y}) = \frac{1}{\sqrt{\alpha^2 - \beta^2}} \times \exp[\gamma(\alpha - \sqrt{\alpha^2 - \beta^2})], \qquad (33)$$

as given below:

$$A = \int_0^\infty dx\, z_k^x \exp(-\frac{2x}{\rho_k}) \times I_0\left[\frac{2}{\rho_k}\sqrt{(m + x)x}\right]$$

$$= \int_0^\infty dx\, \exp\left[-(\frac{2}{\rho_k} + \hbar\omega_k\beta)x\right] \times I_0\left[\frac{2}{\rho_k}\sqrt{(m + x)x}\right]$$

$$= \frac{1}{\sqrt{a_k}} \exp\left[\frac{m}{2}\{\frac{2}{\rho_k} + \hbar\omega_k\beta - \sqrt{a_k}\}\right], \qquad (34)$$

and substituted back to Eq. (32) to obtain:

$$\Delta E_{Ph}^+ = \sum_k \hbar\omega_k z_k^{-\frac{1}{2}} \rho_k^{-1} \frac{1}{\sqrt{a_k^{(1)}}}(1 - z_k) \int_0^\infty dm\, m\, \exp(-\frac{m}{\rho_k}) \exp\left[\frac{m}{2}\{\frac{2}{\rho_k} + \hbar\omega_k\beta - \sqrt{a_k^{(1)}}\}\right]$$

$$= \sum_k \hbar\omega_k z_k^{-\frac{1}{2}} \rho_k^{-1} \frac{1}{\sqrt{a_k^{(1)}}}(1 - z_k) \int_0^\infty dm\, m \exp\left[\frac{m}{2}\{\hbar\omega_k\beta - \sqrt{a_k^{(1)}}\}\right]. \qquad (35)$$

where $a_k^{(1)} = \beta^2\hbar^2\omega_k^2 + 4\beta\hbar\omega_k\rho_k^{-1}$.

The final form of phonon energy transfer for k th mode in the creation process after substituting the standard integration[22]

$$\int_0^\infty dy\, y\, \times \exp(-ay) = \frac{1}{a^2}, \qquad (36)$$

over m with analytical simplification becomes:

$$\Delta E_k^+ = \frac{4\hbar\omega_k}{\rho_k\sqrt{a_k^{(1)}}}(1-z_k)z_k^{-\frac{1}{2}}(\beta\hbar\omega_k - \sqrt{a_k^{(1)}})^{-2} \tag{37a}$$

and similarly, the expression for annihilation processes appears,

$$\Delta E_k^- = -\frac{4\hbar\omega_k}{\rho_k\sqrt{a_k^{(1)}}}(1-z_k)z_k^{-\frac{1}{2}}(\beta\hbar\omega_k + \sqrt{a_k^{(1)}})^{-2}. \tag{37b}$$

Therefore, we find the total energy transfer from the incoming molecule to phonon modes as,

$$\Delta E_{Ph} = \Delta E_{Ph}^+ + \Delta E_{Ph}^- = \sum_k \hbar\omega_k\rho_k\frac{\sin h(\Delta_k)}{\Delta_k}, \tag{38}$$

where $\Delta_k = \frac{1}{2}\hbar\omega_k\beta$. It is quite important to note that energy transfer due to the initial state distribution of the phonon nodes with **BP factor** appears to be surface temperature independent.

When we consider the **Bose - Einstein probability (BEP) factor** for the initial state distribution and substitute Eq. (10), (27) and (28) in the Eq. (26), the expression of energy transfer for creation processes appears as:

$$\begin{aligned}\Delta E_{Ph}^+ &= \sum_k \hbar\omega_k\rho_k^{-1}\sum_{n_k}\sum_{n_k^0}(n_k - n_k^0)(z_k^{n_k^0} + z_k^{2n_k^0} + z_k^{3n_k^0} + z_k^{4n_k^0} + \cdots)\\ &\times \exp[-(n_k + n_k^0 + 1)/\rho_k] \times I_0\left[\frac{2}{\rho_k}\sqrt{(n_k + \frac{1}{2})(n_k^0 + \frac{1}{2})}\right],\end{aligned} \tag{39}$$

which can be simplified to

$$\begin{aligned}\Delta E_{Ph}^+ &= \sum_k \hbar\omega_k\rho_k^{-1}\sum_m m\ \exp(-\frac{m}{\rho_k})\sum_{n_k^0}(z_k^{n_k^0} + z_k^{2n_k^0} + z_k^{3n_k^0} + z_k^{4n_k^0} + \cdots)\\ &\times \exp[-(2n_k^0 + 1)/\rho_k]I_0\left[\frac{2}{\rho_k}\sqrt{(m + n_k^0 + \frac{1}{2})(n_k^0 + \frac{1}{2})}\right],\end{aligned} \tag{40}$$

with $m = n_k - n_k^0$. The double sum in Eq. (40) can be replaced by a double integral to obtain an intermediate result:

$$\begin{aligned}\Delta E_{Ph}^+ &= \sum_k \hbar\omega_k\rho_k^{-1}\int_0^\infty dm\ m\ \exp(-\frac{m}{\rho_k})\int_0^\infty dn_k^0\ (z_k^{n_k^0} + z_k^{2n_k^0} + z_k^{3n_k^0} + z_k^{4n_k^0} + \cdots),\\ &\times \exp[-(2n_k^0 + 1)/\rho_k] \times I_0\left[\frac{2}{\rho_k}\sqrt{(m + n_k^0 + \frac{1}{2})(n_k^0 + \frac{1}{2})}\right],\end{aligned} \tag{41}$$

which turns into the following expression under substitution, $x = n_k^0 + \frac{1}{2}$:

$$
\begin{aligned}
\Delta E_{Ph}^+ &= \sum_k \hbar\omega_k \rho_k^{-1} \int_0^\infty dm\ m\ \exp(-\frac{m}{\rho_k}) \int_0^\infty dx\ (z_k^{x-\frac{1}{2}} + z_k^{2x-1} + z_k^{3x-\frac{3}{2}} + z_k^{4x-2}\cdots) \\
&\quad \times\ \exp[-\frac{2x}{\rho_k}] \times I_0\left[\frac{2}{\rho_k}\sqrt{(m+x)x}\right],
\end{aligned}
\tag{42}
$$

The above standard integrals[22], Eq(33) and Eq(36), are substituted in Eq(42), integrated over x and m and simplified analytically to obtain the final form of phonon energy transfer for k th mode in the creation process as:

$$
\Delta E_k^+ = \hbar\omega_k \rho_k^{-1} \sum_{n=1}^\infty 4a_k^{(n)-\frac{1}{2}} z_k^{-\frac{n}{2}}\left[n\hbar\omega_k\beta - \sqrt{a_k^{(n)}}\right]^{-2},
\tag{43a}
$$

and similarly, the expression for annihilation processes appears,

$$
\Delta E_k^- = -\hbar\omega_k \rho_k^{-1} \sum_{n=1}^\infty 4a_k^{(q)-\frac{1}{2}} z_k^{-\frac{n}{2}}\left[n\hbar\omega_k\beta + \sqrt{a_k^{(n)}}\right]^{-2},
\tag{43b}
$$

where

$$
a_k^{(n)} = n^2\beta^2\hbar^2\omega_k^2 + 4n\beta\hbar\omega_k\rho_k^{-1}.
$$

Thus, the total phonon energy is expressed as:

$$
\Delta E_{Ph} = \Delta E_{Ph}^+ + \Delta E_{Ph}^- = \sum_k k_B T_s \rho_k \sum_{n=1}^\infty \frac{x_k^n}{n},
\tag{44}
$$

where $x_k = \exp(\frac{1}{2}\hbar\omega_k\beta)$.

Thus, the energy transfer due to the inclusion of **BEP factor** for the initial state distribution of the phonon modes brings the surface temperature dependence.

IV. Additional results

In Fig. 6, we display the theoretically calculated reaction probabilities of the incoming H_2 molecule with initial state $v = 1$ and $j = 0$ as function of different initial kinetic energies considering rigid surface and the surface including phonon modes at different temperatures. These results for (a) Cu(100) surface with 300K and 1000K, (b) Cu(110) surface with 190K and 1000K, and (c) Cu(111) surface with 120K and 925K are compared with the corresponding experimentally measured sticking probabilities. The figures clearly demonstrate that the calculated quantities lower estimate the experimental probabilities for all collisional energies

except at lower and higher limits, and remain temperature independent. Fig. 7 depicts the vibrational survival ($v' = 1$) and de - excitation ($v' = 0$) probabilities as function of initial kinetic energies for rigid surfaces and the surfaces [Cu(1nn)] with different temperatures. Those figures show that the elastic/inelastic transition probabilities undergo noticeable change from the rigid surface to the surface including phonon modes with different temperatures for various surface planes (1nn). Fig. 8, 9 and 10 present the rovibrational elastic/inelastic transition probabilities as function of initial kinetic energies for the copper surface with 100, 110 and 111 planes, respectively and indicate substantial difference from rigid surface to the surface with various temperatures. It is quite reasonable to explain the temperature independent sticking probabilities (see Fig. 6) and substantially temperature dependent transition probabilities (see Fig. 7 - 10) in term of phonon energy transferred from the diatom to the solid as functions of time (see Fig. 11) for different collisional energies and as functions of initial kinetic energies (see Fig. 12) with various surface temperatures. In case of $H_2(v = 1, j = 0)$ - Cu(1nn) systems, the amount of overall energy transferred due to the inclusion of phonon modes for specific initial collisional energy and temperature appears enough to increase the transition probabilities but not the sticking probabilities.

Acknowledgment

References

[1] G. D. Billing and S. Adhikari, *Chem. Phys. Lett.*, 2000, **321**, 197.

[2] S. Adhikari and G. D. Billing, *J. Chem. Phys.*, 2000, **113**, 1409.

[3] B. Barkakaty and S. Adhikari, *J. Chem. Phys.*, 2003, **118**, 5302.

[4] P. Puzari, S. Deshpande, S. Adhikari, *Chem. Phys.*, 2004, **300**, 305.

[5] P. Puzari, S. Adhikari, *Int. J. Quant. Chem.*, 2004, **98**, 434.

[6] P. Puzari, B. Sarkar and S. Adhikari, *J. Chem. Phys.*, 2004, **121**, 707.

[7] P. Puzari, B. Sarkar and S. Adhikari, *Int. J. Quantum Chem.*, 2005, **105**, 209.

[8] P. Puzari, R. S. Swathi, B. Sarkar and S. Adhikari, *J. Chem. Phys.*, 2005, **123**, 134317.

[9] P. Puzari, B. Sarkar, S. Adhikari, *Chem. Phys.*, 2006, **324**, 497.

[10] P. Puzari, B. Sarkar and S. Adhikari, *J. Chem. Phys.*, 2006, **125**, 194316.

[11] S. Sardar, A. K. Paul, P. Mondal, B. Sarkar and S. Adhikari, *Phys. Chem. Chem. Phys.*, 2008, **10**, 6388.

[12] S. Sardar, A. K. Paul, R. Sharma and S. Adhikari, *J. Chem. Phys.*, 2009, **130**, 144302.

[13] S. Sardar, A. K. Paul and S. Adhikari, *Mol. Phys.*, 2009, **107**, 2467.

[14] S. Sardar, A. K. Paul, R. Sharma and S. Adhikari, *Int. J. Quantum Chem.*, DOI:10.1002/qua.22578.

[15] S. Sardar, P. Puzari and S. Adhikari, *Chem. Phys. Lett.*, 2010, **496**, 341.

[16] P. A. M. Dirac, *Proc. Cambridge Philos. Soc.*, 1930, **26**, 376.

[17] G. Wiesenekker, G. J. Kroes and E. J. Baerends, *J. Chem. Phys.*, 1996, **104**, 7344.

[18] A. Salin, *J. Chem. Phys.*, 2006, **124**, 104704.

[19] C. Díaz, E. Pijper, R. A. Olsen, H. F. Busnengo, D. J. Auerbach and G. J. Kroes, *Science*, 2009, **326**, 832.

[20] G. C. Schatz, F. J. McLafferty and J. Ross, *J. Chem. Phys.*, 1977, **66**, 3609.

[21] G. D. Billing, B. C. Eu and C. Nyeland, *Chem. Phys.*, 1978, **29**, 427.

[22] I. S. Gradshteyn and J. M. Ryzhik, *Table of integrals, series and products*, Academic Press, New York, 1965.

[23] H. A. Michelsen and D. J. Auerbach, *J. Chem. Phys.*, 1991, **94**, 7502.

[24] C. T. Rettner, H. A. Michelsen and D. J. Auerbach, *J. Chem. Phys.*, 1995, **102**, 4625.

Table I The barrier heights (E_b) and their locations (r_b and Z_b) are given for H_2 dissociating with its molecular axis kept parallel to the Cu(1nn) surface. The numbers in the parenthesis are the results of Wiesenekker *et al.*[17], Salin *et al.*[18] and Díaz *et al.*[19] for Cu(100), Cu(110) and Cu(111) surfaces, respectively.

	Impact site	Dissociation to	E_b (eV)	r_b (Å)	Z_b (Å)
Cu(100)	bridge	hollow	0.50 (0.48)	1.22 (1.23)	1.05 (1.05)
	hollow	bridge	0.55 (0.63)	1.20 (1.00)	1.17 (1.14)
	top	bridge	1.10 (0.72)	1.35 (1.43)	1.45 (1.40)
	bridge	top	1.23 (1.37)	1.88 (2.09)	1.52 (1.52)
Cu(110)	top	short bridge	1.25	1.37	1.45
	short bridge	hollow	0.72 (0.63)	1.22	1.00
Cu(111)	bridge	hollow	0.38 (0.63)	1.08 (1.03)	1.30 (1.17)
	top	bridge	0.80 (0.89)	1.32 (1.40)	1.48 (1.39)

Figure caption

Fig. 1. Top view of the (a) Cu(100), (b) Cu(110) and (c) Cu(111) surfaces consist of 133, 134, 134 atoms, respectively. First, second and third layer are indicated by circle, square and triangle, respectively.

Fig. 2. The contour plot of EDIM - fit ground adiabatic PES for H_2 interacting on bridge site and dissociating to hollow site of (a) Cu(100), (b) Cu(110) and (c) Cu(111) surface, respectively.

Fig. 3. Average distance ($\langle Z(t) \rangle$) from the centre of mass position of the $H_2(v{=}0, j{=}0)$ to the top layer of the Cu(100) surface and bond length ($\langle r(t) \rangle$) of diatom as functions of time (a) for collisional energy 0.40 eV with higher (solid line) and lower (dashed line) number of basis functions, whereas (b) for collisional energy 0.70 eV with ImA_Z values 2.0 amu τ^{-1} (solid line) and 0.1 amu τ^{-1} (dashed line) including higher number of basis functions only.

Fig. 4. (a) and (b) display the energy transfer (ΔE_{Ph}) from $H_2(v = 0, j = 0)$ to Cu(100) and Cu(110) surfaces , respectively as functions of time at two different temperatures.

Fig. 5. (a) and (b) display the energy transfer (ΔE_{Ph}) at asymptotic time from $H_2(v = 0, j = 0)$ to Cu(100) and Cu(110) surfaces , respectively as functions of collision energy at two different temperatures.

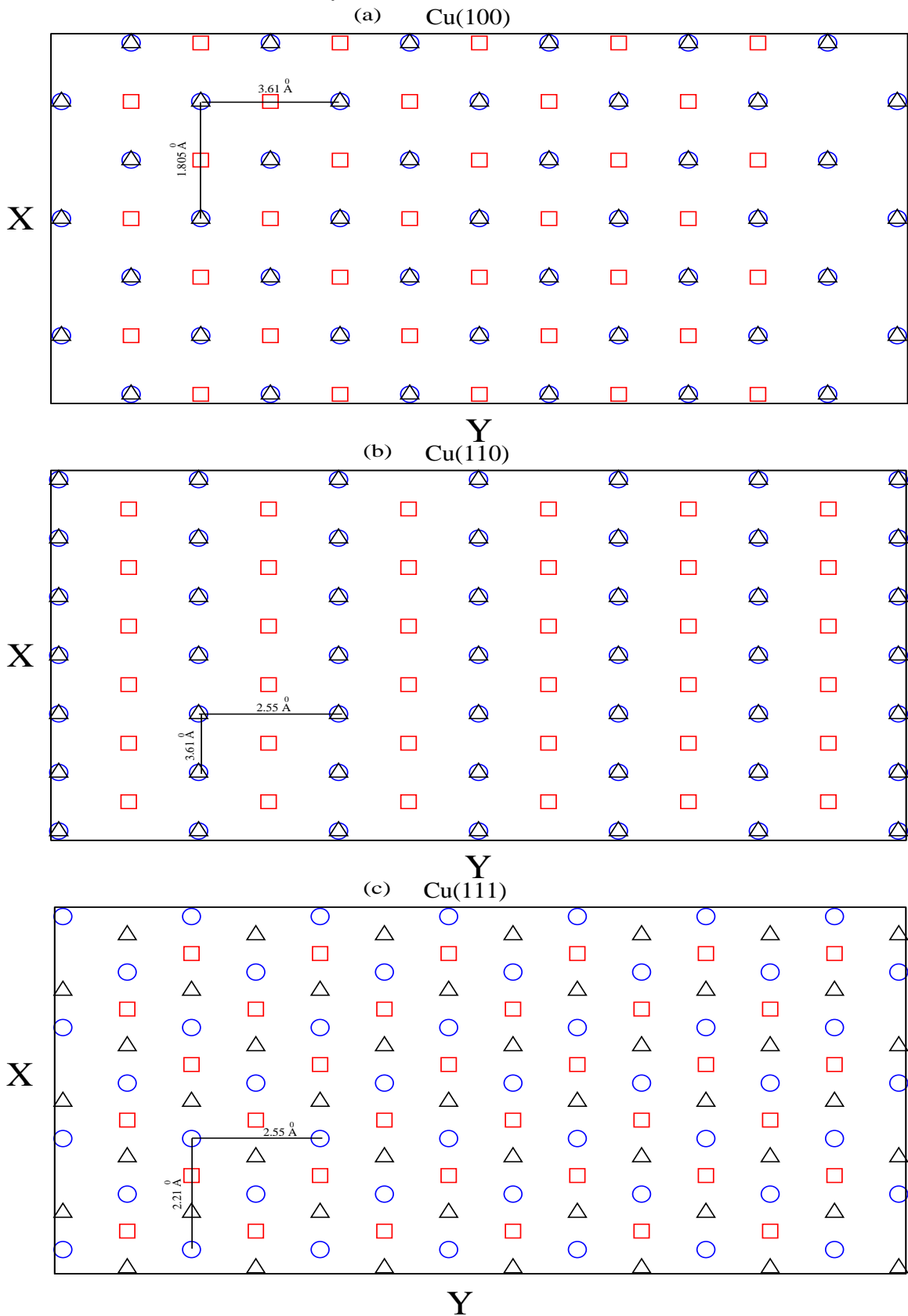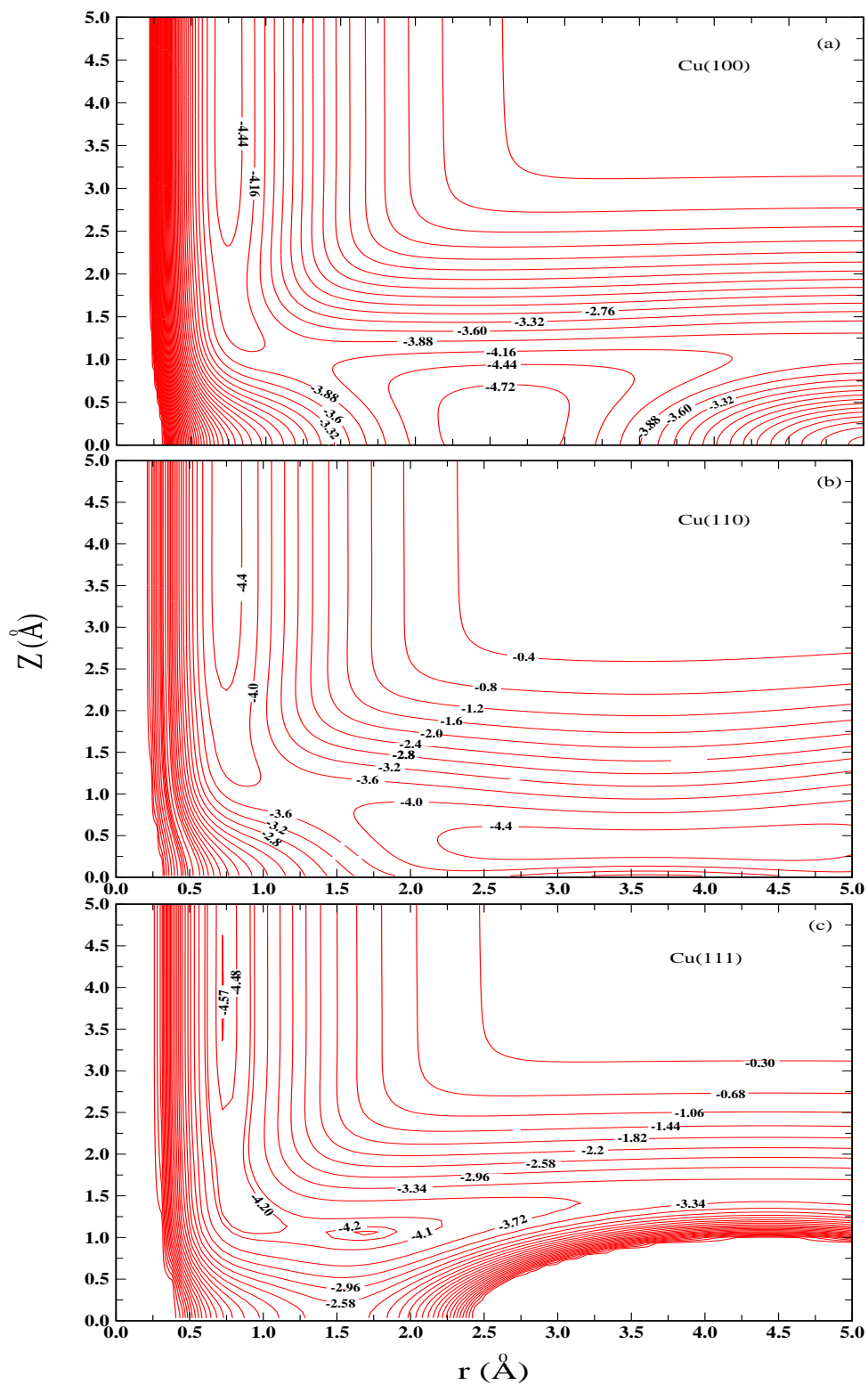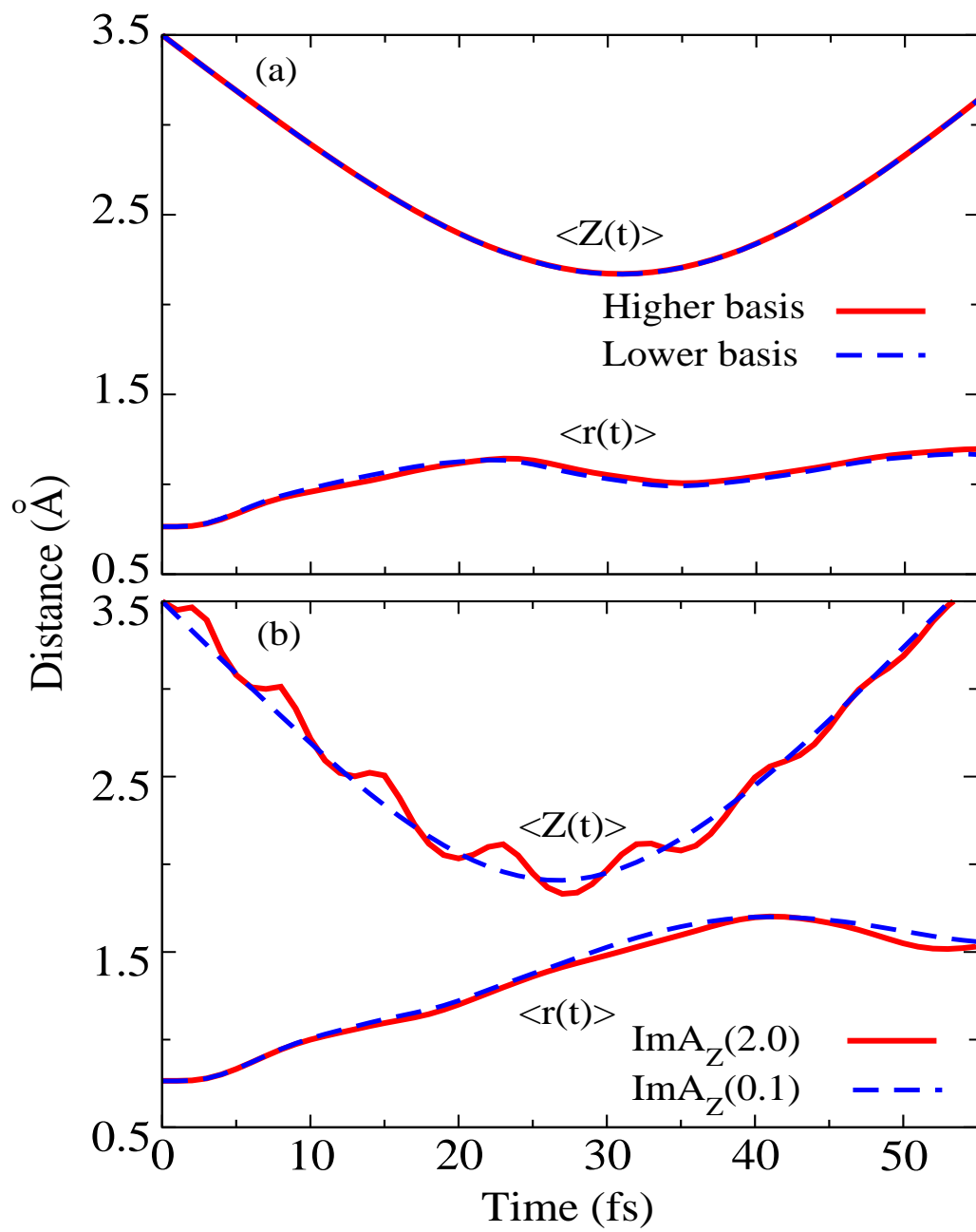Fig. 6. Calculated sticking probability($P_{Stick}(E)$) for $H_2(v = 1, j = 0)$ on Cu(100), Cu(110) and Cu(111) surfaces as functions of initial collisional energy are presented in panel (a), (b) and (c), respectively, whereas experimental results are obtained from Ref. [23, 24].

Fig. 7. The energy resolved state - to - state transition probabilities for vibrationally inelastic, $v{=}1 \rightarrow v' = 0$ (solid line) and elastic, $v{=}1 \rightarrow v' = 1$ (dashed line) collision as functions of collisional energy of the diatom on Cu(100), Cu(110) and Cu(111) surfaces are presented in

panel (a), (b) and (c), respectively.

Fig. 8. In case of Cu(100) plane, the calculated state - to - state rovibrational transition probabilities (v=1, j=0 $\rightarrow$ v', j') are shown in (a) v'=0, j'=0; (b) v'=0, j'=2 ; (c) v'=0, j'=4; (d) v'=1, j'=0; (e) v'=1, j'=2; (f) v'=1, j'=4 for rigid surface and two different surface temperatures.

Fig. 9. In case of Cu(110) plane, the calculated state - to - state rovibrational transition probabilities (v=1, j=0 $\rightarrow$ v', j') are shown in (a) v'=0, j'=0; (b) v'=0, j'=2 ; (c) v'=0, j'=4; (d) v'=1, j'=0; (e) v'=1, j'=2; (f) v'=1, j'=4 for rigid surface and two different surface temperatures.

Fig. 10. In case of Cu(111) plane, the calculated state - to - state rovibrational transition probabilities (v=1, j=0 $\rightarrow$ v', j') are shown in (a) v'=0, j'=0; (b) v'=0, j'=2 ; (c) v'=0, j'=4; (d) v'=1, j'=0; (e) v'=1, j'=2; (f) v'=1, j'=4 for rigid surface and two different surface temperatures.

Fig. 11. (a), (b) and (c) display the energy transfer (ΔE_{Ph}) from $H_2(v = 1, j = 0)$ to Cu(100), Cu(110) and Cu(111) surfaces , respectively as functions of time at two different temperatures.

Fig. 12. (a), (b) and (c) display the energy transfer (ΔE_{Ph}) at asymptotic time from $H_2(v = 1, j = 0)$ to Cu(100), Cu(110) and Cu(111) surfaces , respectively as functions of collision energy at two different temperatures.
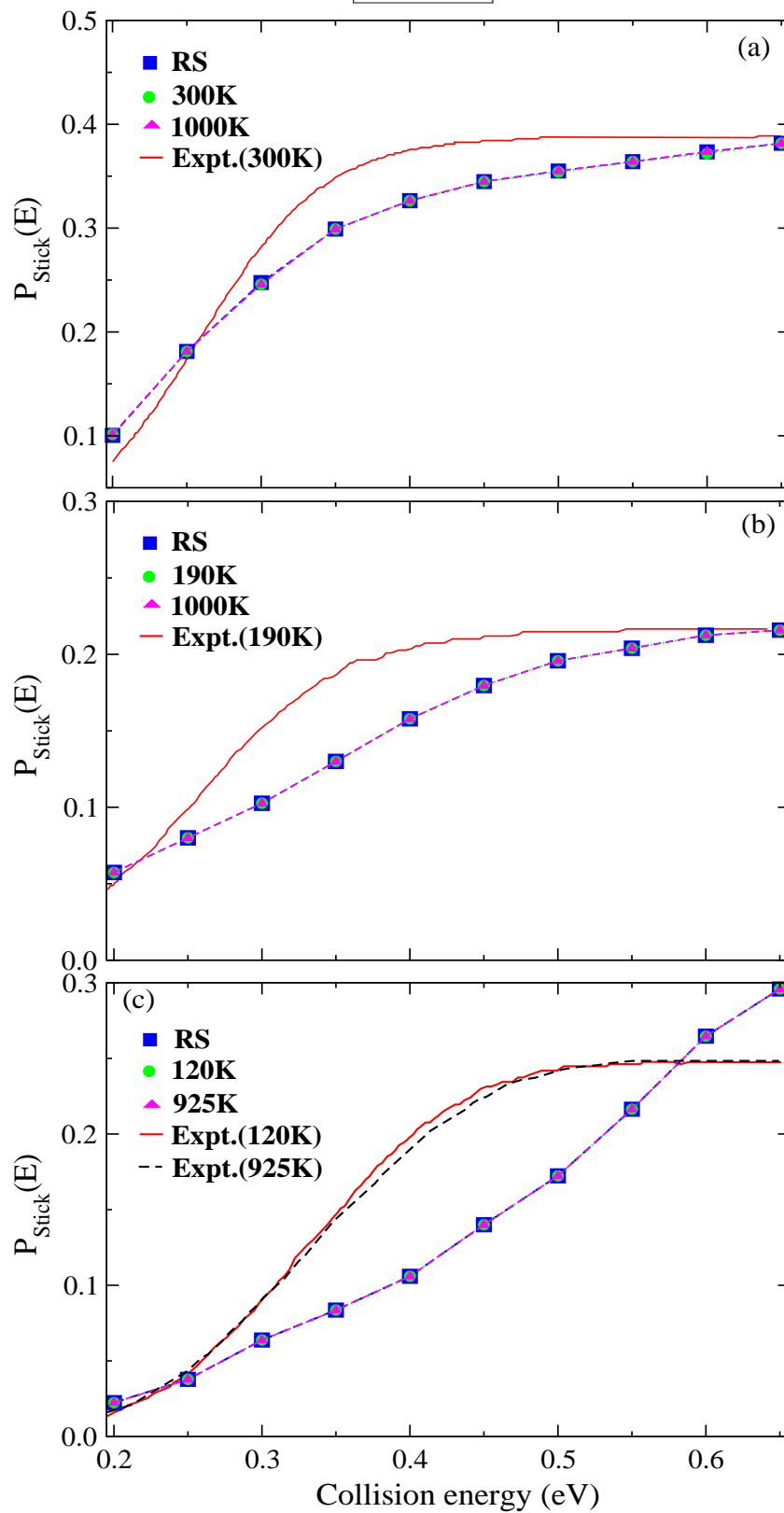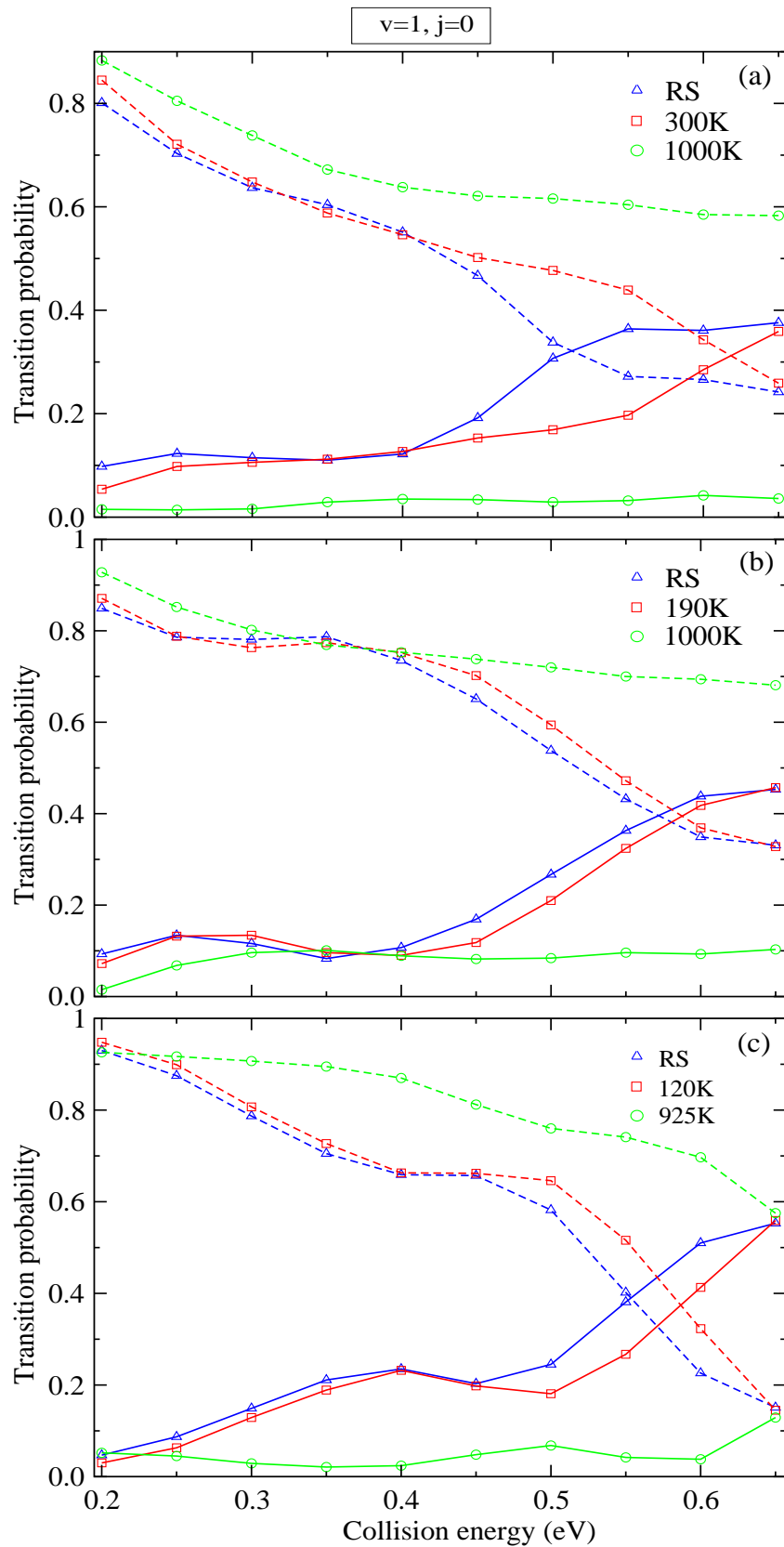
(a)   Cu(100)

(b)   Cu(110)

(c)   Cu(111)

Fig. 1.

Fig. 2.

20

Fig. 3.
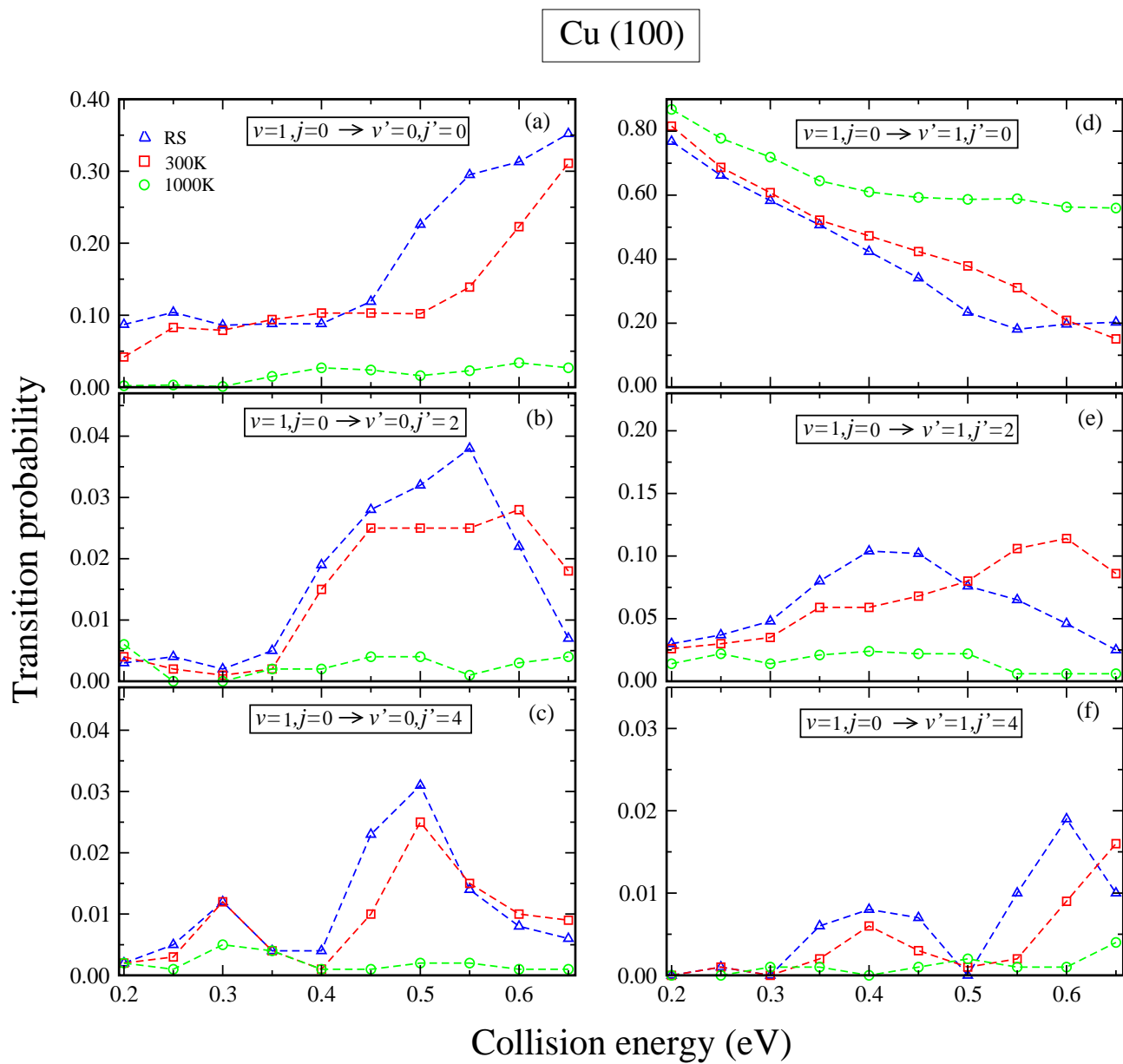
Fig. 4.

Fig. 5.

Fig. 6.

v=1 , j=0
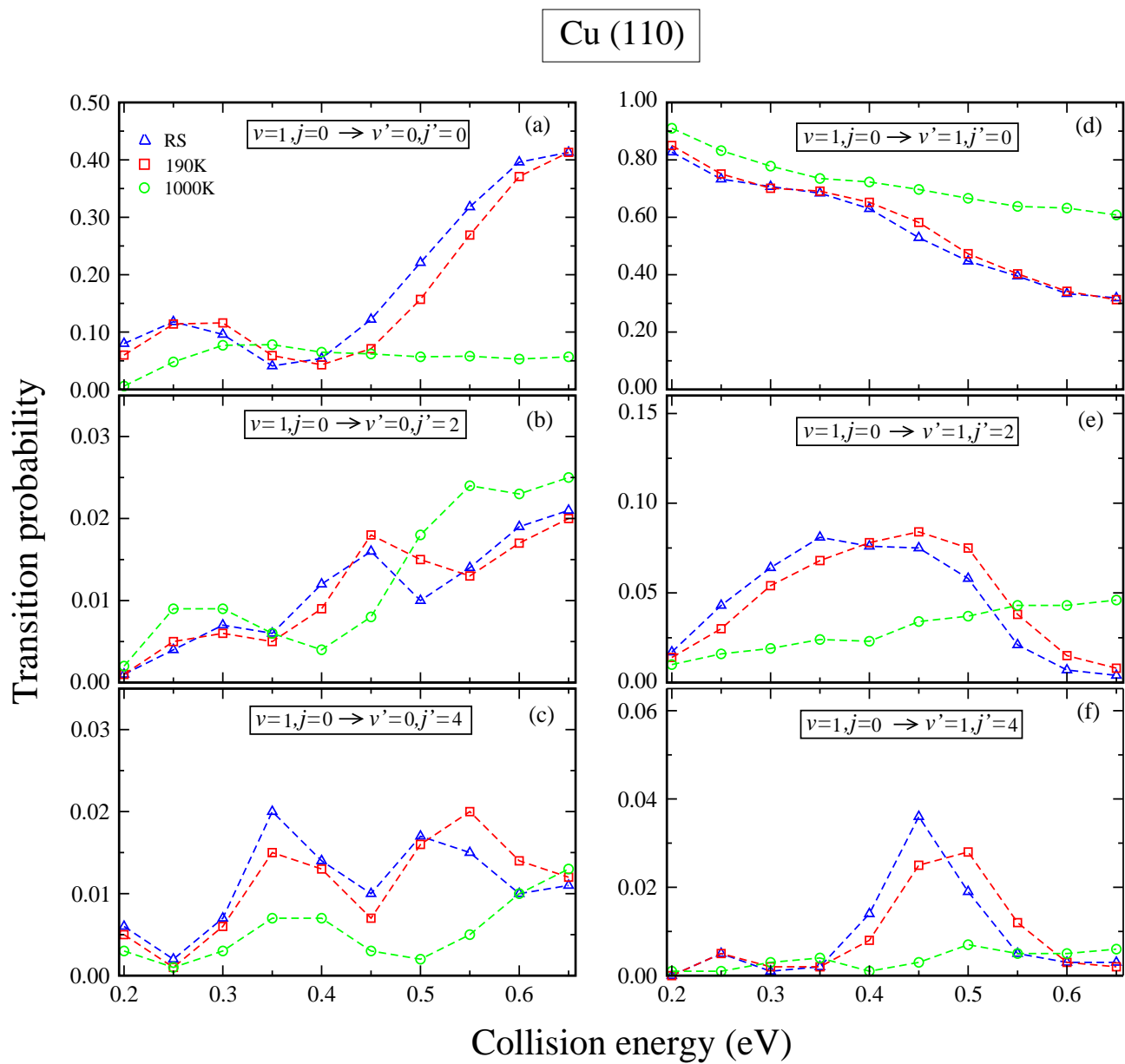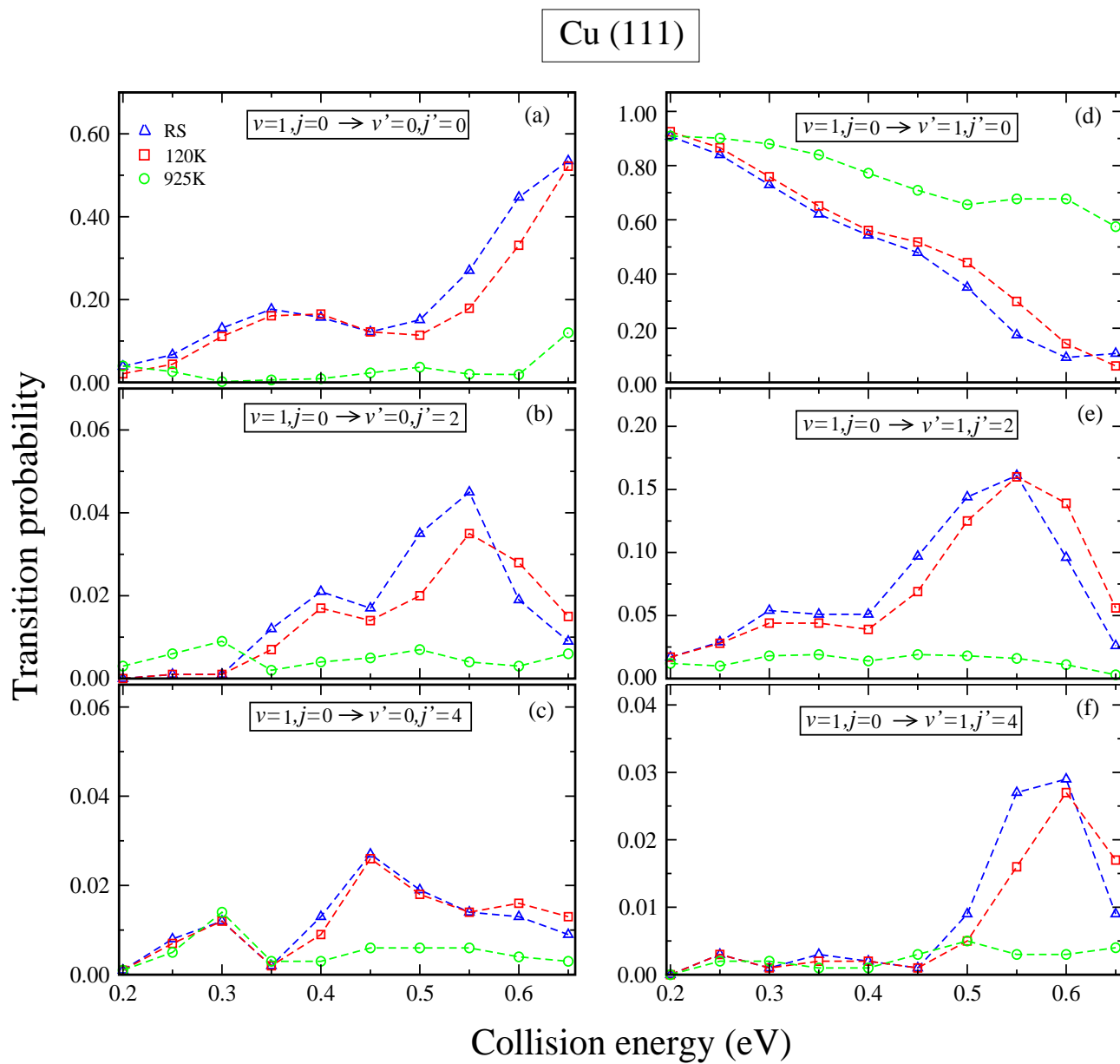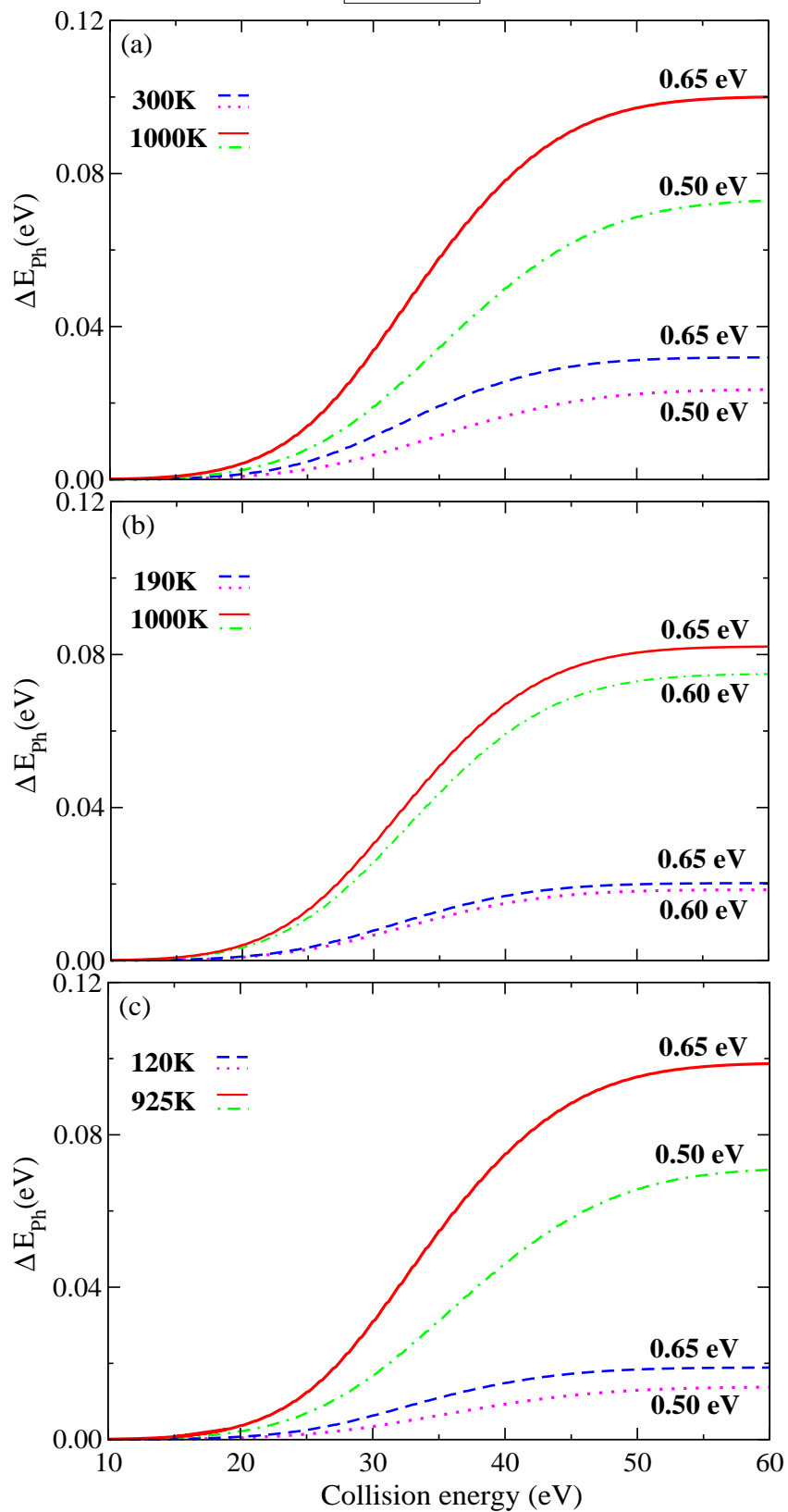

Fig. 7.

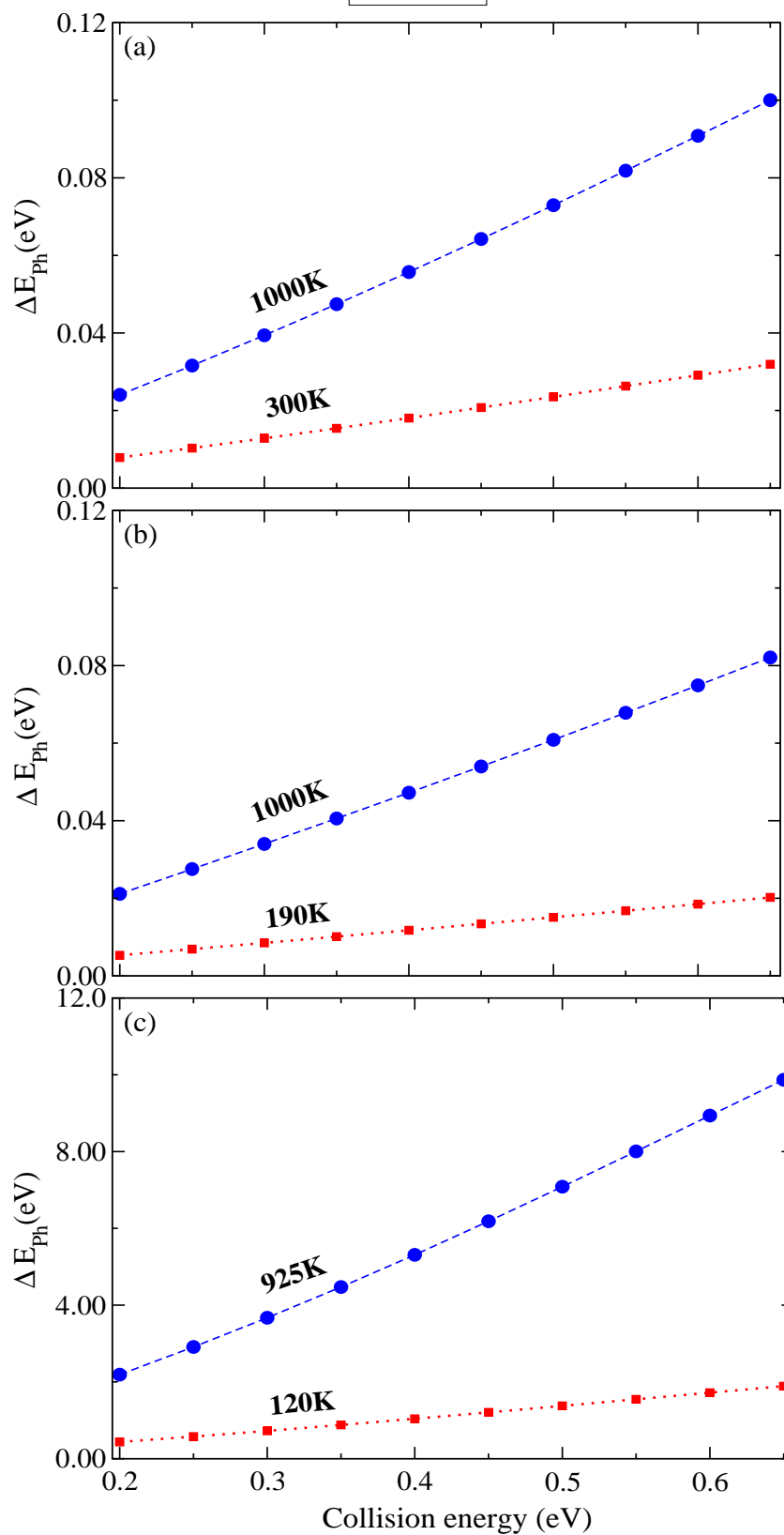Cu (100)

Fig. 8.

Cu (110)
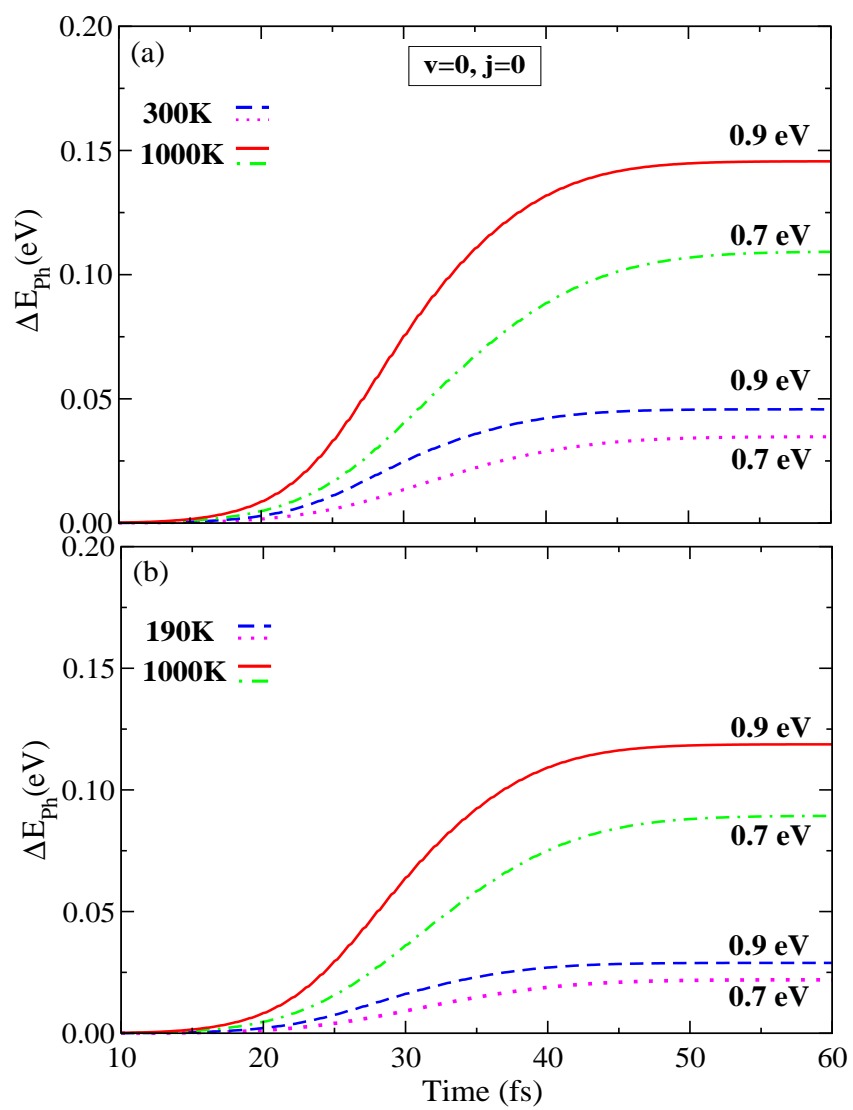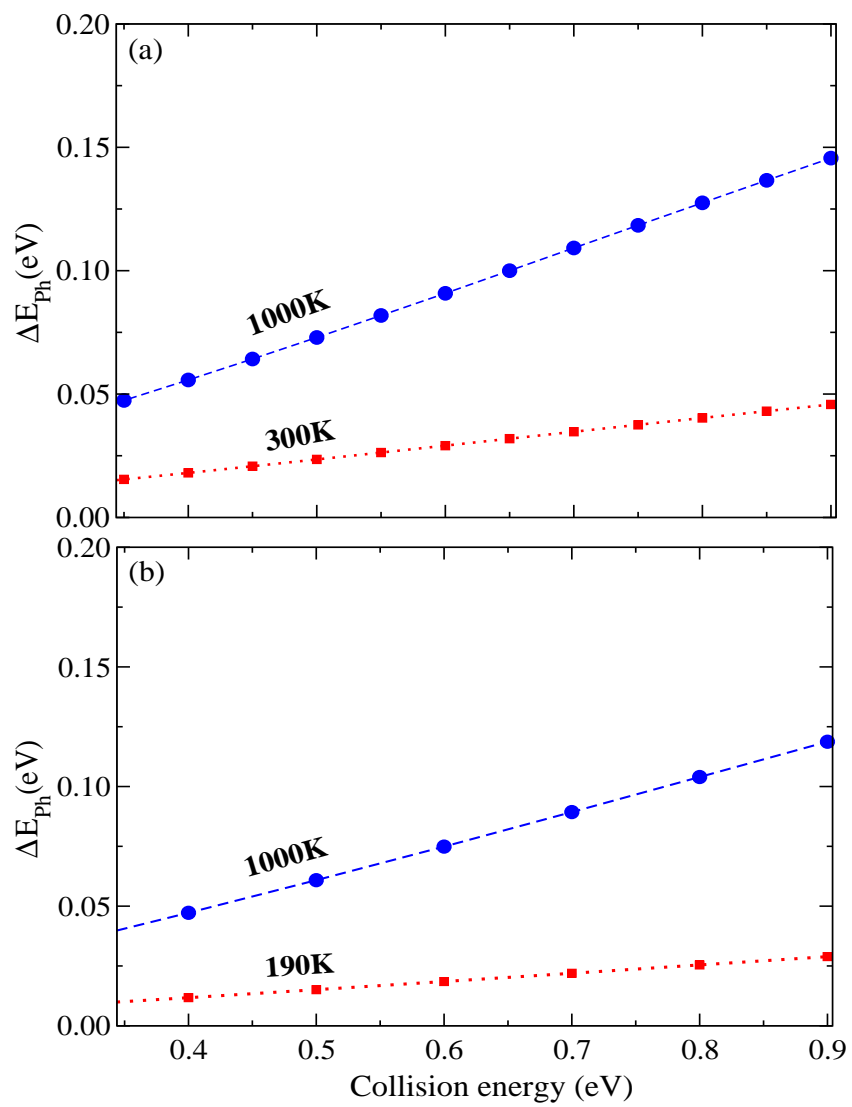
Fig. 9.

Fig. 10.

$v=1, j=0$

Fig. 11.

$v=1, j=0$

Fig. 12.